Synthesis, Cocrystallization, and Enzymatic Degradation of Novel Poly(butylene-*co*-propylene succinate) Copolymers

George Z. Papageorgiou and Dimitrios N. Bikiaris*

Laboratory of Organic Chemical Technology, Department of Chemistry, Aristotle University of Thessaloniki, GR-541 24, Thessaloniki, Macedonia, Greece

Received March 19, 2007; Revised Manuscript Received May 23, 2007

A series of poly(butylene-*co*-propylene succinate) (PBPSu) random copolyesters were synthesized and characterized using ^{1}HNMR spectroscopy and viscometry. Tensile properties decreased with increasing propylene succinate (PSu) content. Cocrystallization and multiple melting behaviors were investigated. The copolymers showed a eutectic behavior. The minimum melting point corresponded to 75 mol % PSu. Wide-angle X-ray diffraction (WAXD) patterns showed that the copolymers with up to 60 mol % PSu units formed poly(butylene succinate) crystals. The interplanar spacings slightly differentiated. The copolymer with 11.5 mol % poly(propylene succinate) (PPSu) units formed PPSu crystals. The results indicated isodimorphic cocrystallization. The cocrystallization was thermodynamically analyzed using the Wendling−Suter model. The defect free energy decreased for copolymers with high PPSu content. The banded spherulites of the copolyesters were studied, and growth rates were analyzed using the Lauritzen−Hoffman theory. Enzymatic hydrolysis study, using *Rhizopus delemar* and *Pseudomonas cepacia* lipases, showed that degradation was faster for copolymers with high PSu content, compared even to the fast-degrading PPSu.

Introduction

Aliphatic polyesters such as poly(L-lactic acid), poly(ϵ-caprolactone), poly(butylene succinate) (PBSu), poly(3-hydroxy butyrare), poly(3-hydroxy valerate), and so forth, due to their favorable features of biodegradability and biocompatibility, make up a very important class of biodegradable polymers. Nowadays they are available commercially in a variety of forms used for several applications. Last years they attracted considerable attention, and numerous research works have been published, especially on polyhydroxyalkanoates, which are the most studied among biodegradable polyesters.[1−7]

PBSu is one of the most promising biodegradable polyesters, since it has high mechanical properties. Its crystal structure, crystallization, and melting behavior have been reported.[6−14] Recently, different types of copolymers and blends of PBSu have been studied.[15−29] Papers dealing with composites and ionomers based on PBSu have also appeared.[30,31] The polymer shows sufficient tensile properties and stability against thermal degradation; however, it exhibits a slow biodegradation rate as a result of its high degree of crystallinity.[32]

Poly(propylene succinate) (PPSu) is a relatively new biodegradable polymer that exhibits high biodegradation rates and is also produced using monomers from renewable resources.[33−39] It had been difficult to prepare since one of its monomers, 1,3-propanediol (PD) could not be produced until recently in sufficient quantities and purity.[35,36] PPSu has gained increasing interest, since it has a higher biodegradation rate compared to that of poly(ethylene succinate) and PBSu and also degrades faster than poly(propylene adipate) and poly(propylene sebacate) and maybe faster than most of the polymers due to its low crystallinity.[40−41] In contrast to other biodegradable polyesters, a limited number of published works dealing with PPSu have been reported.[13,33−46] Unfortunately, PPSu has low mechanical properties. Copolymers or blends with balanced enzymatic degradation/mechanical properties might fulfill demands in applications; however, works on copolymers or blends of PPSu are really rare.[29,44,45]

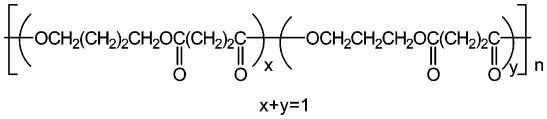

Figure 1. Chemical structure of PBPSu copolymers. *x* and *y* are the molar fractions for BSu and PSu units in the copolymers, respectively.

Basic research on the relationship between structure, morphology, and properties as well efforts to understand the biodegradation mechanism will enable us to design and synthesize a great variety of biodegradable polymers to fulfill the demands in practical applications.[1] Biodegradation rate is undoubtedly one of the most important properties of aliphatic polyesters. The enzymatic degradation of polyesters is sensitive to their chemical structure, the hydrophilic/hydrophobic balance within the main chain, molecular weight, the specific solid-state morphology, crystallinity, and so forth. As for crystalline structure and morphology, spherulite size and lamellar structure can greatly influence the rate of biodegradation.[1,22,27]

For copolymers, it is known that higher degradation rates can be achieved relative to that of homopolymers, and this is basically attributed to the limited crystallinity.[1] In most of the copolymers where both components are crystallizable, the degree of crystallinity decreases as the minor component content increases as a result of the incompatibility in crystal lattices of the two components.[47,48] On the contrary, if the two crystallizable units are compatible in each crystal lattice, cocrystallization can take place. Two cases of cocrystallization behavior have been reported. For components with similar chemical structure, isomorphism may occur, meaning that only one crystalline phase containing both comonomer units is observed at all compositions. In isodimorphism, two crystalline phases

* Corresponding author. Tel.: +30 2310 997812. Fax: +30 2310 997769. E-mail address: dbic@chem.auth.gr.

10.1021/bm0703113 CCC: $37.00
Published on Web 07/27/2007

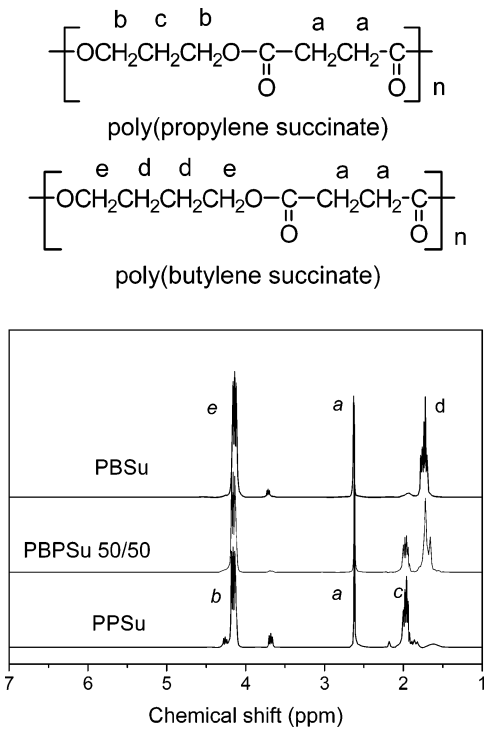

Figure 2. Chemical structures of PBSu and PPSu showing the different hydrogen atom groups, and ^{1}HNMR spectra for the two homopolymers and the PBPSu 50/50 copolymer.

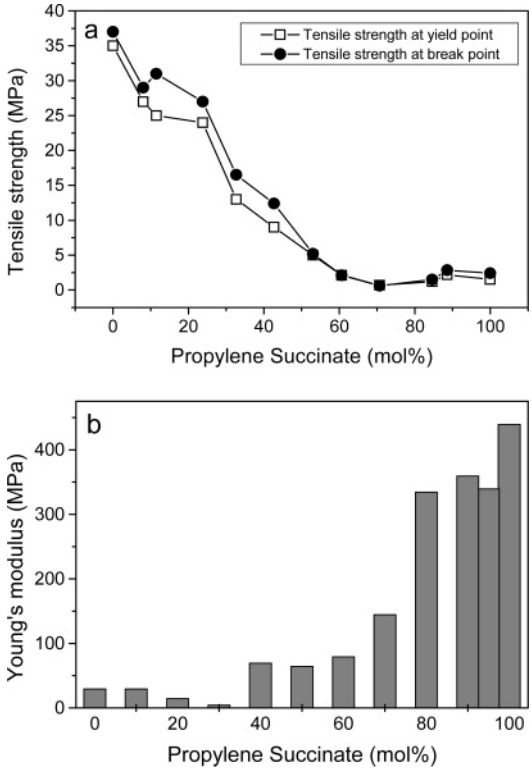

Figure 3. Mechanical properties of PBPSu copolymers.

and pseudo-eutectic behavior are observed. Isodimorphism has been observed in most cases of random copolymers.[15,18,49−52] Various models have been proposed, among them those of Flory, Sanchez−Eby, Baur, and recently, Wendling and Suter, to describe in thermodynamic terms the cocrystallization of copolymers.[53−63]

As was reported above, PPSu has fast crystallization rates, but, unfortunately, it exhibits low mechanical properties. The aim of this study was to synthesize a complete series of fully biodegradable poly(butylene-*co*-propylene succinate) (PBPSu) copolymers in order to produce polyesters with high biodegradation rates and satisfactory mechanical properties. Synthesis of such a series has not been reported before. On the other hand, despite their importance, combined analyses of both the enzymatic degradation and solid-state structure of a full series of biodegradable copolymers, especially succinate copolyesters, are missing from the literature. In general, in most cases where the synthesis of such new copolymer series is reported, solid-state studies are in fact limited to standard characterization. An effort was made in this work to carry out detailed studies of the effect of the progressive variation in copolymer composition on both the enzymatic degradation and the solid structure. Thus, in this paper, apart from the synthesis and the enzymatic hydrolysis behavior of high molecular weight PBPSu's, melting behavior, thermodynamic analysis of cocrystallization, crystallization kinetics, and spherulitic morphology examination are presented.

Experimental

Materials. The polyesters and copolyesters were synthesized from succinic acid and the proper diol or mixture of diols. Succinic acid (purum 99%) and butylene glycol (purum 99%) were purchased from Aldrich Chemical Co. PD (CAS Number: 504-63-2, Purity: >99.7%) was kindly supplied by Du Pont de Nemours Co. Tetrabutyl titanate catalyst of analytical grade and polyphosphoric acid (PPA) used as a heat stabilizer were purchased from Aldrich Chemical Co. All the other materials and solvents that were used for the analytical methods were of analytical grade.

The aliphatic polyesters were prepared by the two-stage melt polycondensation method (esterification and polycondensation) in a glass batch reactor. In brief, the proper amount of succinic acid and appropriate glycols in an acid/diol molar ratio of 1:1.1 and the catalyst $Ti(OBu)_4$ were charged into the reaction tube of the polyesterification apparatus. The apparatus with the reagents was evacuated several times and filled with argon in order to remove all of the oxygen. The reaction mixture was heated at 190 °C under an argon atmosphere and stirred at a constant speed (500 rpm). This first step (esterification) is considered complete after the collection of a theoretical amount of H_2O, which is removed from the reaction mixture by distillation and collected in a graduate cylinder.

In the second step of polycondensation, PPA was added (5×10^{-4} mol PPA/mol succinic acid), which is believed to prevent side reactions such as etherification and thermal decomposition. A vacuum (5.0 Pa) was applied slowly over a period of time of about 30 min, to avoid excessive foaming and to minimize oligomer sublimation, which is a potential problem during the melt polycondensation. The temperature was slowly increased to 230 °C while the stirring speed was increased to 720 rpm. The polycondensation continued for about 60 min for all prepared polyesters. After the polycondensation reaction was completed, the polyesters were easily removed, milled, and washed with methanol.

Nuclear Magnetic Resonance (NMR). ^{1}H NMR spectra of polyesters were obtained with a Bruker AMX 400 spectrometer operating at a frequency of 400 MHz for protons. Deuterated chloroform ($CDCl_3$) was used as solvent in order to prepare solutions of 5% w/v. The number of scans was 10, and the sweep width was 6 kHz.

Intrinsic Viscosity Measurement. Intrinsic viscosity [η] was measured using an Ubbelohde viscometer at 25 °C in chloroform.

Gel Permeation Chromatography (GPC). GPC analysis was performed using a Waters 150C GPC equipped with a differential refractometer as a detector and three Ultrastyragel (103, 104, and 105 Å) columns in series. $CHCl_3$ was used as the eluent (1 mL/min), and the measurements were performed at 35 °C. Calibration was performed using polystyrene standards with a narrow molecular weight distribution.

Table 1. Composition of Diol Mixture in Reactor Feed, Copolymer Composition Determined by ^{1}HNMR, Intrinsic Viscosity (IV) Values, Number Average Molecular Weight (M_n), Heat of Fusion (ΔH_m), and Degree of Crystallinity (X_c) of PBPSu Copolymer Samples

polyester code	IV, cdL/g	M_n, g/mol	BD/PD molar ratio in feed	BSu/PSu molar ratio in copolymer	ΔH_m, J/g	X_c, % (X-ray)
PBSu	0.57	16900	100.0/0.0	100.0/0.0	92.7	45.1
PBPSu 95/5	0.70	20830	94.6/5.4	92.0/8.0	85.2	42.3
PBPSu 90/10	0.62	18050	89.2/10.8	88.5/11.5	75.4	32.1
PBPSu 80/20	0.64	18780	78.6/21.4	76.2/23.8	51.7	26.5
PBPSu 70/30	0.77	23560	68.2/31.8	67.3/32.7	36.2	23.4
PBPSu 60/40	0.67	18940	57.9/40.1	57.3/42.7	30.5	21.8
PBPSu 50/50	0.65	18900	47.9/52.1	47.0/53.0	28.3	19.6
PBPSu 40/60	0.66	19360	38.0/62	39.4/60.6	22.1	13.4
PBPSu 30/70	0.73	21880	28.2/71.8	29.1/70.7	0.0	0.0
PBPSu 20/80	0.73	21340	18.7/81.3	15.1/84.6	0.0	0.0
PBPSu 10/90	0.61	17800	9.3/90.7	11.4/88.6	28.6	22.1
PPSu	0.63	18630	0.0/100.0	0.0/100.0	35.6	25.6

Thermal Analysis. A Perkin−Elmer, Pyris 1 differential scanning calorimeter (DSC), calibrated with indium and zinc standards, was used. Samples of 5 ± 0.1 mg were used in the tests. They were sealed in aluminum pans and heated to 30 °C above the melting point at a heating rate of 20 °C/min. The samples were held at that temperature for 5 min in order to erase any thermal history. For isothermal crystallizations, the sample was cooled by 200 °C/min to 20 °C above the crystallization temperature and finally cooled to the crystallization temperature at a rate 50 °C/min to achieve equilibration of the instrument. The heating rate was, in most tests, 20 °C/min. The cases in which some other rate was used are discussed in the specified section. Fresh sample was used in each run.

Wide-Angle X-ray Diffraction Patterns (WAXD). X-ray diffraction measurements of the samples were performed by an automated powder diffractometer (PW 1050) with Bragg−Brentano geometry ($\theta-2\theta$), using CuK_α radiation ($\lambda = 0.154$ nm) in the 2θ angle range of 5−60°.

Mechanical Properties. Measurements of tensile mechanical properties were performed on an Instron 3344 dynamometer in accordance with ASTM D638 using a cross-head speed of 50 mm/min. From the films prepared, dumb-bell shaped tensile-test specimens (central portions 5 × 0.5 mm thick, 22 mm gauge length) were cut in a Wallace cutting press and conditioned at 25 °C and 55−60% relative humidity for 48 h. The values of elongation at break and tensile strength were determined. At least five specimens were tested for each sample, and the average values are reported.

Enzymatic Hydrolysis. Polyesters in the form of films 5 × 5 cm in size with approximately 2 mm thickness, prepared by melt-pressing using a hydraulic press, were placed in Petri dishes containing phosphate buffer solution (pH 7.2) with 0.09 mg/mL *Rhizopus delemar* lipase and 0.01 mg/mL of *Pseudomonas cepacia* lipase. The Petri dishes were then incubated at 30 ± 1°C in an oven for several days while the media were replaced every 3 days. After a specific period of incubation (every 72 h), the films were removed from the Petri dish, washed with distilled water, and weighted until a constant weight was reached. The degree of biodegradation was estimated from the mass loss.

Scanning Electron Microscopy (SEM). The morphology of the prepared films before and after enzymatic hydrolysis was examined in a Jeol (JMS−840) SEM system equipped with an energy-dispersive X-ray Oxford ISIS 300 microanalytical system. The films were covered with a carbon coating in order to have good conductivity of the electron beam. Operating conditions were as follows: accelerating voltage, 20KV; probe current, 45 nA; and counting time, 60 s.

Polarizing Light Microscopy (PLM). A polarizing optical microscope (Nikon, Optiphot-2) equipped with a Linkam THMS 600 heating stage, a Linkam TP 91 control unit, and a Jenoptic ProgRes C10plus camera with the Capture Pro 2.1 software was used for PLM observations.

Results and Discussion

Characterization of Copolymers. The homopolyesters and the copolyesters were synthesized following the two-step polycondensation method described in the experimental section. The composition of the copolyesters was estimated from the ^{1}HNMR spectra using the relative intensities of the proton peaks arising from butylene succinate (BSu) and propylene succinate (PSu) repeating units. Figure 2 shows the ^{1}HNMR spectra for the two homopolymers and the 50/50 w/w copolymer (reactor feed composition). The ^{1}H NMR spectrum of PPSu showed a single peak at 2.63 ppm attributed to methylene protons of succinic acid (*a* protons), a triple peak 4.09−4.21 ppm attributed to *b* protons, and a multiple peak between 1.9 and 2.02 ppm corresponding to *c* protons. The PBSu ^{1}H NMR spectrum has many similarities and showed the characteristic peaks of succinic acid and the important multiple peak at 1.8−2 ppm attributed to *d* proton groups. The peak positions in the copolymer spectrum were identical to those for the homopolymers. The molar composition of the PBPSu copolymers was calculated as the area ratio of peaks for *c* protons of PPSu and *d* protons of PBSu according to eq 1. Four *d* protons appear in the BSu repeating unit, while two *c* protons appear in the PSu unit. Thus, the area for *c* protons was multiplied by a factor 2 in eq 1. The results are summarized in Table 1. In general, there is only a small deviation from the feed composition. In the following discussion, however, the samples will be referenced using the weight ratio of the diols in the feed composition for simplicity.

$$\frac{X_{PSu}}{X_{BSu}} = \frac{2c}{d} \quad (1)$$

The molecular weight distribution of the prepared polyesters was determined from the intrinsic viscosity values as well as by GPC. It can be seen from Table 1 that the synthesized copolymers have very similar molecular weights. However, as can be seen in Figure 3, there is a direct dependence of the mechanical properties on the copolymer composition. As the amount of BSu units increased in the copolymers, the tensile strength at break as well as the Young's modulus increased, although the variation did not follow a linear function. For high PSu amounts (50−90 mol %), the tensile strength and Young's modulus were very low and almost identical to those of the neat PPSu. This is because PPSu is a soft material, and, because of the high concentrations of PSu units in the copolymers, their sequences dominated. Furthermore, as it will be discussed in

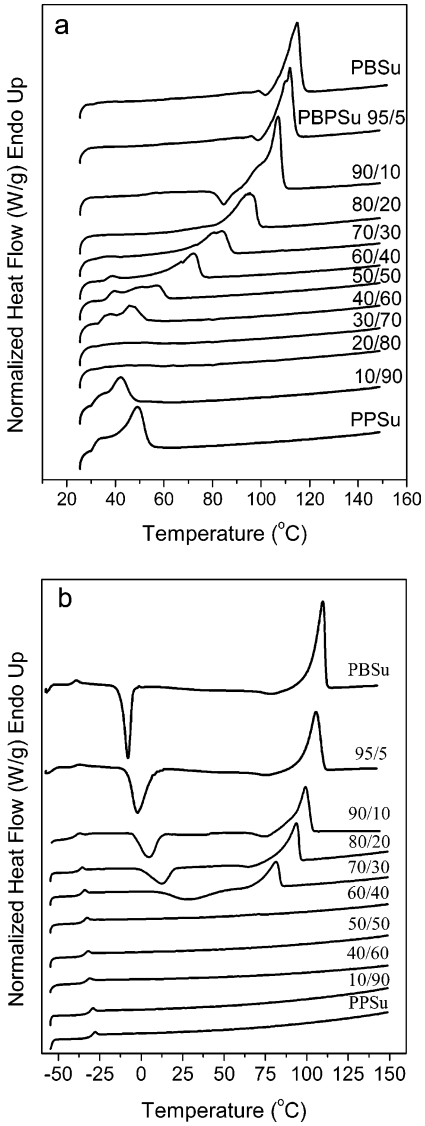

Figure 4. DSC traces for PBSu, PPSu, and copolyester (a) as-received and (b) quenched samples.

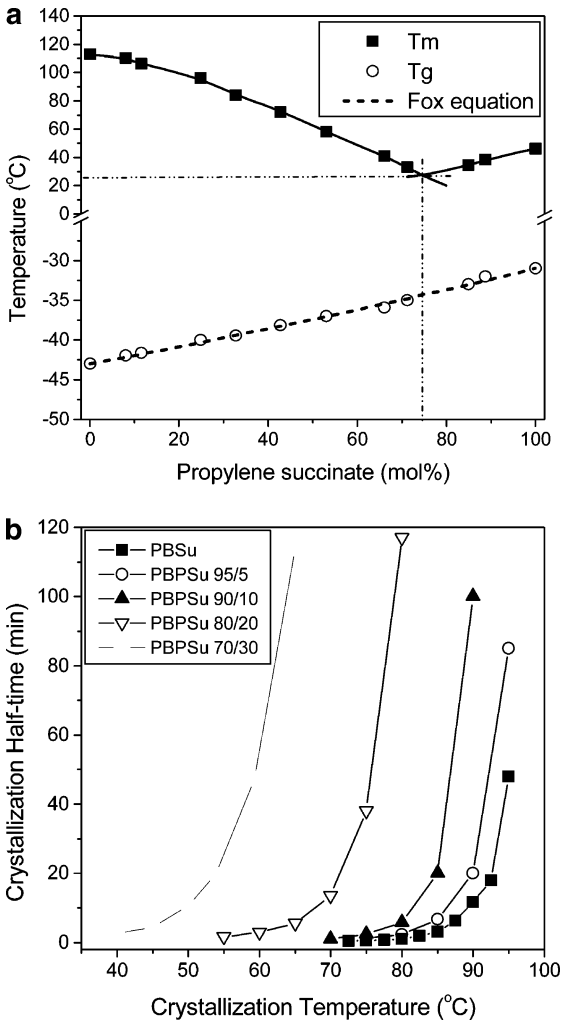

Figure 5. (a) Variation of the melting point and the glass transition temperature for the PBPSu copolymers and (b) crystallization half-times for PBSu- and BS-rich copolymers measured from isothermal experiments from the melt.

the following, the copolymers with PSu amounts of about 70 and 80 mol % were completely amorphous and very soft materials, and this fact affected the mechanical properties negatively. By increasing the BSu content, the mechanical properties progressively increased, approximating those values for PBSu.

Thermal analysis carried out with DSC showed that the homopolyesters and most of copolyesters were semicrystalline. Figure 4a shows the DSC traces for the as-received samples of PBSu and PBSu-rich copolymers. As can be seen, the polymers crystallized during cooling and storage at room temperature, but, as a matter of fact, copolymers with intermediate composition showed broad or multiple melting peaks on heating scans. Also, the melting points and heat of fusion decreased with comonomer content. PBPSu 30/70 and 20/80 were amorphous.

Figure 4b shows the DSC traces for the quenched copolymer samples. In these traces, a clear glass transition can be seen for the copolymers. For the neat PBSu and the corresponding copolymers with high BSu units, a cold crystallization accompanied the glass transition.

Figure 5 shows the variation of the melting point and glass transition temperature with increasing PSu content in the copolyesters. A systematic melting point depression is observed with increasing the comonomer unit content, showing a pseudo-eutectic behavior. The melting point of the 30/70 and 20/80 copolymers after prolonged crystallization at 0 °C was found to be slightly higher than room temperature. The as-received samples of the specific copolymers did not show any melting peak, since crystallization at room conditions was impossible. The minimum melting point does not appear at the equimolar composition, but it corresponds to 75 mol % PSu content and 27 °C.

The glass transition temperatures (T_g) of quenched samples, on the other hand, increased monotonically with PSu content between the two values for the neat polymers, which were −43 °C for PBSu and −31 °C for PPSu for the homopolymer samples of this work. In amorphous random copolymers, T_g is usually a monotonic function of composition, and the most common relationship used to predict T_g as a function of comonomer content is the equation of Fox:[64]

$$\frac{1}{T_g} = \frac{w_1}{T_{g1}} + \frac{w_2}{T_{g2}} \tag{2}$$

where w_1 and w_2 are the weight fractions of the comonomers, and T_{g1} and T_{g2} are the glass transition temperatures of the respective homopolymers. As can be seen in Figure 5, the equation of Fox describes well the variation of the glass transition temperatures of the copolymers.

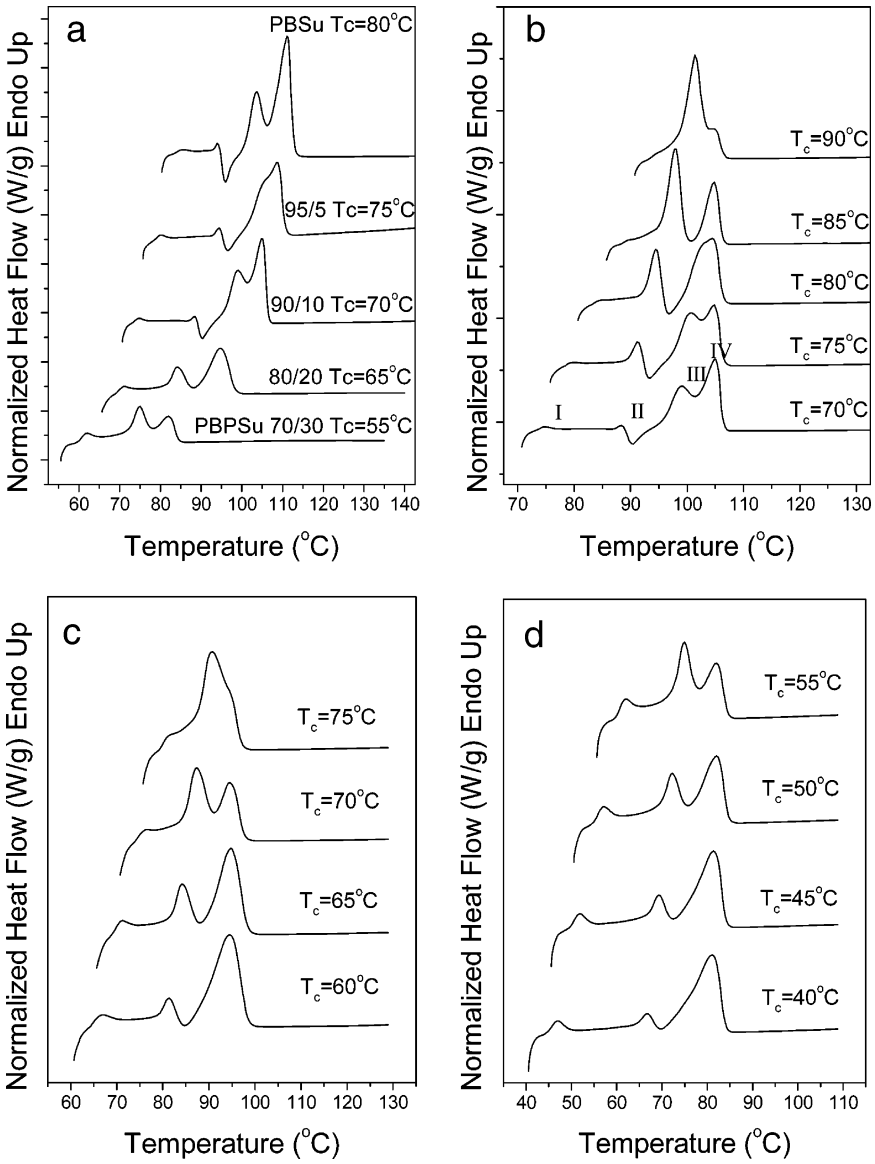

Figure 6. DSC heating scans for (a) PBPSu copolymers isothermally crystallized from the melt at the same supercooling, (b) PBPSu 90/10, (c) PBPSu 80/20, and (d) PBPSu 70/30 samples isothermally crystallized from the melt at different temperatures. Heating rate 20 °C/min.

For the PPSu and those copolyesters with high PSu unit content, crystallization is very slow, and no cold-crystallization occurred during the heating scan with 20 °C/min. Isothermal experiments verified the slow crystallization rates for these samples. In contrast, PBSu and copolymers in which BSu units are dominating crystallized fast. Figure 5b shows the crystallization half-times for PBSu- and BSu-rich copolymers. As one can see, there is an increase in the crystallization half-times, showing retardation in the phenomenon with increasing comonomer unit content. Also, the temperature window for crystallization shifts to lower temperatures, and it becomes narrower. This is because the melting point is reduced, but also there is a need for increased supercooling, as the comonomer units reduce symmetry along the macromolecular chains and may act as noncrystallizing segments or form crystal defects if they are incorporated into the crystals.

Multiple Melting Behavior. DSC traces for various copolymers isothermally crystallized from the melt at about the same supercooling ($\Delta T = T_m - T_c \approx 30$ °C) are shown in Figure 6a. Figure 6b shows the melting traces for the PBPSu 90/10 copolymer samples. Similar to PBSu, multiple melting behavior can be observed in general for its copolyesters. Up to four melting peaks and also a recrystallization exotherm can be observed in the heating scans by 20 °C/min for PBPSu 90/10. The first peak appears at about 10 °C above the crystallization temperature and is marked as peak I. Furthermore, peak I appeared only after increased crystallization time. Peak I is the so-called annealing peak and is usually associated with the melting of secondary crystals, although another interpretation is that this is associated with the balance of the melting and recrystallization processes.[13,65,66] The second peak appears before recrystallization. This is marked as peak II. For high heating rates, peak II shifted to a higher temperature and also dominated with increasing T_c. Thus, it is due to the melting of original crystals. Two more peaks appear after the recrystallization exotherm in the DSC traces, marked as III and IV in order of increasing temperature. Peak III was not always observed, as it shifted to higher temperature with increasing crystallization temperature and finally coincided with the ultimate peak IV. The latter was not affected by increasing crystallization temperature T_c. In contrast, peaks I and II increased in peak temperature with increasing T_c. The heat of fusion corresponding to peaks III and IV was reduced when T_c was increased, in contrast to that of peak II. For slow heating rates, extended

recrystallization occurred as well as an increased number of melting peaks, and the temperature of the ultimate peak increased as a result of longer time available for crystal perfection during the scans. In general, a continuous perfection process such as that via melting and recrystallization should be appropriate for the interpretation of the phenomena. This was also reported for the neat PBSu and PPSu.[10−14] After all, peaks III and IV should be associated with the melting of recrystallized material, and not with original crystals. For copolymers, the probability for the existence of defects in crystals is, by definition, much higher because of the occurrence of the comonomer units along the crystallizable segments. A higher portion of secondary crystals should be supposed, as well as a decrease in the copolymer crystal size, increasing free energy and reducing the stability of the crystalline phase. This is verified not only by the drop in T_m, but also by the fact that the relative intensity of peak I is higher for copolymers with higher comonomer content, as it is clearly seen in Figure 6c,d, especially for the traces for PBPSu 70/30. The recrystallization peak became less obvious with increasing comonomer content and finally for PBPSu 70/30 almost disappeared, although the DSC traces corresponded to samples crystallized under the same supercooling. This shows that recrystallization for copolymers with high PSu content is slower, and further that the possibility of crystal perfection is limited. Also, in general, as can be seen, the total heat of fusion was lower for the copolymers, despite the fact that the crystallization process was complete in every case. The ultimate achievable crystallinity value was reduced with increasing comonomer content, as can be seen in Table 1 for the as-received samples.

Cocrystallization Behavior. In most of the copolyesters where both A and B components are crystallizable, the degree of crystallinity decreases as the minor component content increases, leading often to fully amorphous materials even at low comonomer compositions. This is due to incompatibility in the crystal lattices of the two components. On the contrary, if the two crystallizable units are compatible in each crystal lattice, cocrystallization can take place. Two cases of cocrystallization behavior have been reported.[47,48] For components with similar chemical structure, isomorphism may occur. In isomorphism, since the two components occupy about the same volume, the excess free energy of cocrystallization is small. Thus, the chain conformations of both corresponding homopolymers are compatible with either crystal lattice, and only one crystalline phase is observed at all compositions. This crystalline phase contains both comonomer units. Isomorphism is evidenced by a clear melting temperature or by some crystallinity over the entire copolymer composition. On the other hand, in isodimorphism, two crystalline phases are observed. The isodimorphism is also subdivided into two cases. In the former case, each crystalline phase contains comonomer units: the incorporation of B units in A crystal lattices and vice versa. In the other case, the A units can cocrystallize with the incorporation of the B comonomeric units, whereas B crystallizes with the complete rejection of the A units. In both cases of isodimorphism, the increase of minor comonomer concentration in each crystalline phase results in lowering of the melting temperature and the crystallinity of copolymer. Thus, pseudo-eutectic behavior is an evidence for isodimorphism, that is, a minimum melting temperature is observed in the plot of melting temperature versus copolymer composition.

The monomeric units of PBSu and PPSu are very similar. This might enable cocrystallization. For PBSu, it is known that α-crystal modification is monoclinic with unit cell dimensions

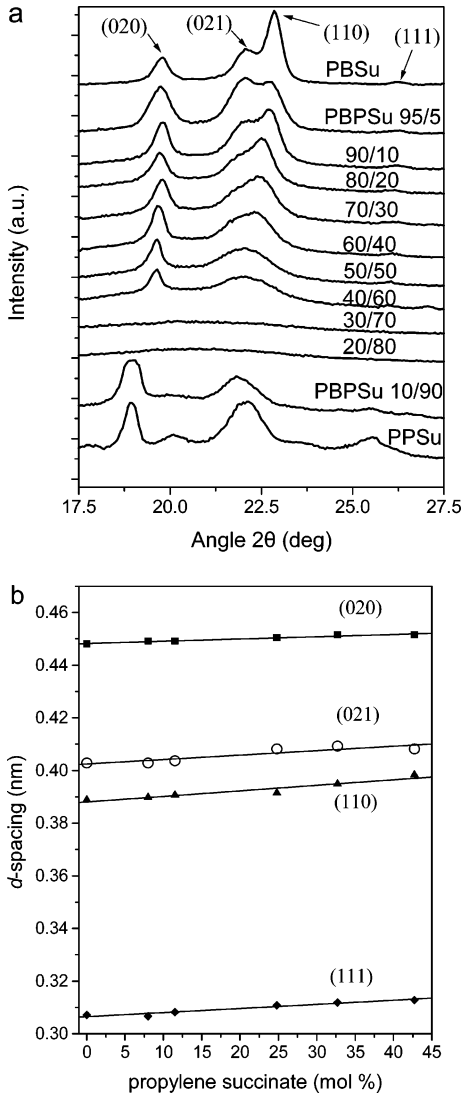

Figure 7. (a) WAXD patterns for PBSu, PPSu, and the PBPSu copolyesters and (b) interplanar *d*-spacings as a function of copolymer composition.

$a = 0.521$ nm, $b = 0.914$ nm, $c = 1.094$ nm, and $\beta = 124°$.[6−8] For PPSu, the crystal lattice parameters have not been reported up to now. However, for polymers with an odd number of methylene groups in the glycol or in the acid part, the unit cell is expected to be orthorhombic, in contrast to those with an even number of methylene groups, which all crystallize with a monoclinic unit cell.[67] To check the nature of the crystalline phase in the polymers under investigation, a WAXD study was performed. Comonomer concentration in the crystal lattice is strongly dependent on the copolymer composition in bulk and the crystallization conditions. In Figure 7a, the WAXD patterns of the PBPSu copolymers are shown. Except for PBPSu 30/70 and 20/80, which were amorphous, in the WAXD patterns, crystalline reflection peaks can be observed. The reflections for the BSu-rich copolymers are those associated with the PBSu α-crystal form; that is, exclusively, PBSu crystals are formed. For PBPSu 10/90, the pattern was very similar to that of neat PPSu, despite the lower crystallinity, and no indication for PBSu crystal was observed (Figure 7a). This means that the formation of PBSu crystals should be excluded for the specific copolymer. It must be noted that, for the rest of the semicrystalline copolymers, including even PBPSu 40/60, the patterns are similar to that for PBSu crystals, although there are some slight shifts in the peak positions, especially for higher comonomer

content, showing the effect of comonomer cocrystallization. These observations combined with the fact that PBPSu copolymers exhibited eutectic behavior lead to the conclusion that these copolymers show isodimorphic cocrystallization. Indications for isodimorphism were also reported for poly(butylene-*co*-ethylene succinate) copolymers.[20] Although for the PBPSu copolymers this could not be directly evidenced, the transition from PBSu to PPSu crystal structure occurs at the composition for which the eutectic point is predicted. PPSu crystallizes hardly due to the propylene segment. The bulkier BSu comonomer content further reduces symmetry along the copolyester chains and three-dimensional order, finally resulting in amorphous materials. Normally, crystallization can occur only for an 11.5 mol % comonomer content or less in PPSu chains. Overall, it seems to be easier for shorter PSu units to be incorporated in the PBSu crystal lattice than it is for the bulkier BSu units to be incorporated in the PPSu lattice. A systematic decrease in the crystallinity is obvious in Table 1, due to the reduction in length of homopolymer sequences and the occurrence of defects. The crystallinity values were calculated from WAXD patterns using the relative areas under the crystalline peaks, A_c, and the amorphous background, A_{am}, using the equation

$$X_c = \left(1 + \frac{A_{am}}{A_c}\right)^{-1} \quad (3)$$

according to Hay et al.[68]

What can be observed in the WAXD patterns (Figure 7) for the copolymers crystallizing in PBSu crystals is the continuous broadening of the peaks corresponding to the (021) and (110) reflections, which also have reduced relative intensities compared to that of the reflection for the (020) plane. These observations should be attributed to the decreased three-dimensional long-range order that occurs when comonomer units are incorporated in the crystals or when the crystal size decreases. As the comonomer concentration in bulk increases, the fraction, which is incorporated in the crystal lattice, increases. The peak positions indicate a slight variation for copolymers with increasing PSu unit content, since they shift to slightly lower 2θ diffraction angles.

For qualitative estimation of the extent of cocrystallization in PBSu crystals, the change in the lattice *d*-spacings in the WAXD patterns was used. When comonomer inclusion occurs, the *d*-spacings vary with the comonomer content. The strong reflections of the PBSu α-form crystals correspond to the (020), (021), (111), and (110) planes. The *d*-spacing of Miller planes seem to increase slightly with comonomer content (Figure 7b). This is a result of the distortion in the crystal lattice due to comonomer inclusion, which should take place for increased comonomer content in the bulk.

Determination of the Equilibrium Melting Temperature. Equilibrium melting temperature (T_m^o) is, by definition, the melting temperature of lamellar crystals with an infinite thickness. Since it is impossible to obtain such a lamella in practice because of kinetic factors, extrapolative methods are used to estimate T_m^o.[69] Among them, the Hoffman−Weeks method has been commonly used and accepted to estimate T_m^o.[70] Despite criticism, the Hoffman−Weeks procedure is still in use because of its simplicity and straightforward experimental implementation. In this procedure, the measured T_m of specimens crystallized at different T_c is plotted against T_c and a linear extrapolation to the line $T_m = T_c$, and the intercept gives T_m^o. The Hoffman−Weeks extrapolation is based on an equation that was deduced from a combination of the Gibbs−Thomson equation and secondary nucleation theory, which will be applied below to analyze spherulitic growth rate data. In this equation,

$$T_m = T_m^o\left(1 - \frac{1}{r}\right) + \frac{T_c}{r} \quad (4)$$

T_m is the observed melting temperature of a crystal formed at a temperature T_c, r is the thickening coefficient equal to l_c/l_g^*, where l_c is the thickness of the grown crystal and l_g^* is the initial thickness of a chain-folded lamellar crystal. The prerequisite for the application of this theory is the isothermal thickening process of lamellar crystals at a specific crystallization temperature and the dependence of the thickening coefficient on the crystallization temperature.

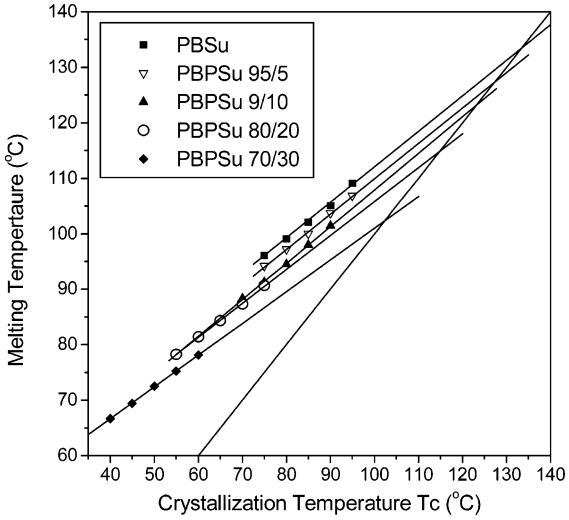

Figure 8. Hoffman−Weeks plots for the determination of the equilibrium melting temperatures of PBSu and PBPSu copolymers with high BSu content.

Table 2. Equilibrium Melting Temperature and Nucleation Parameter Constant Values for PBSu and Copolymers with High BSu Content

polyester code	PSu content, mol %	T_m^o, °C	K_g, 10^{-5} K^2
PBSu	0.0	133.5	1.85
PBPSu 95/5	8.0	126.5	1.58
PBPSu 90/10	11.5	123.2	1.56
PBPSu 80/20	24.8	112.9	1.46
PBPSu 70/30	32.7	107.9	1.37

The T_m^o for PBSu and the PBPSu copolymers with high BSu content were determined following the linear Hoffman−Weeks extrapolation. For PBSu and its copolyesters, as was reported in the respective section, it was found that the melting peak II observed in DSC traces corresponded to primary crystals formed during the isothermal crystallization stage. Thus, the respective melting temperatures T_{mII} were plotted against the crystallization temperature, as shown in Figure 8. Results for the equilibrium melting temperatures (T_m^o) of PBSu and its copolyesters are summarized in Table 2.

Melting Point Depression. The melting point depression of the PBPSu copolymers was analyzed by using the Flory,[53,54] Baur,[55] and Sanchez−Eby[56] equations and the Wendling−Suter[57−59] model for cocrystallization of copolymers of A and B comonomers.

According to Flory,[53,54] in the case of comonomer exclusion, the upper bound of the copolymer melting temperature can be calculated as follows:

$$\frac{1}{T_m^o} - \frac{1}{T_m(X_B)} = \frac{R}{\Delta H_m^o} \ln(1 - X_B) \quad (5)$$

where X_B is the concentration of the minor comonomer B units in the polymer, and $\ln(1 - X_B)$ equals the collective activities of A sequences in the limit of the upper bound of the melting temperature. T_m^o and ΔH_m^o are the homopolymer equilibrium melting temperature and heat of fusion, respectively, and R is the gas constant.

Helfand and Lauritzen[61] and later Sanchez and Eby[56] considered the case of B comonomer units included into the crystals of A where they act as defects and derived the so-called comonomer inclusion models. The Sanchez−Eby equation is

$$\frac{1}{T_m^o} - \frac{1}{T_m(X_B)} = \frac{R}{\Delta H_m^o} \ln(1 - X_B + X_B e^{-\epsilon/RT}) \quad (6)$$

Here, $X_B e^{-\epsilon/RT}$ is the equilibrium fraction of repeat units B that are able to crystallize, and ϵ is the excess free energy of a defect created by the incorporation of one B unit into the crystal.

According to Baur,[55] copolymer crystals can be treated as a "pseudo-eutectic" system, where the homopolymer sequences of length ξ may be included into crystals of lamellar thickness corresponding to that length. The melting point is calculated as follows:

$$\frac{1}{T_m^o} - \frac{1}{T_m(X_B)} = \frac{R}{\Delta H_m^o} [\ln(1 - X_B) - \langle \xi \rangle^{-1}] \quad (7)$$

where $\langle \xi \rangle = [2X_B(1 - X_B)]^{-1}$ is the average length of homopolymer sequences in the melt.

Among the models, the more recent one (that of Wendling and Suter[57−59]) combines the Sanchez−Eby[56] model (a comonomer inclusion model) with the Baur[55] model (a comonomer exclusion model). The Wendling and Suter model is given by

$$\frac{1}{T_m^o} - \frac{1}{T_m(X_B)} = \frac{R}{\Delta H_m^o} \left[\frac{\epsilon X_{CB}}{RT} + (1 - X_{CB}) \ln \frac{1 - X_{CB}}{1 - X_B} + X_{CB} \ln \frac{X_{CB}}{X_B} + \langle \tilde{\xi} \rangle^{-1} \right] \quad (8)$$

where X_{CB} is the concentration of the B units in the crystal.

In the equilibrium comonomer inclusion, the concentration of B units in the crystal is given by

$$X_{CB}^{eq} = \frac{X_B e^{-\epsilon/RT}}{1 - X_B + X_B e^{-\epsilon/RT}} \quad (9)$$

When X_{CB} in eq 8 is substituted by eq 9, eq 8 is simplified to the following equilibrium inclusion model:

$$\frac{1}{T_m^o} - \frac{1}{T_m(X_B)} = \frac{R}{\Delta H_m^o} \{\ln(1 - X_B + X_B e^{-\epsilon/RT}) - \langle \tilde{\xi} \rangle^{-1}\} \quad (10)$$

where

$$\langle \tilde{\xi} \rangle^{-1} = 2(X_B - X_B e^{-\epsilon/RT}) \cdot (1 - X_B + X_B e^{-\epsilon/RT}) \quad (11)$$

When $X_{CB} = X_B$ and $X_{CB} = 0$, eq 8 reduces to the uniform inclusion model and the exclusion model, respectively.

In Figure 9a, the experimental excess crystallization Gibbs energy obtained as $[\Delta H_m^o/(RT_m)] \cdot (1 - T_m/T_m^o)$ is plotted together with the theoretical values calculated as a function of copolymer composition for the copolyesters of this work. The excess free energy was calculated as $\ln(1 - X_B) - \langle \tilde{\xi} \rangle^{-1}$ in the case of the Baur model and $\ln(1 - X_B)$ in the case of the Flory model. Only in the case of copolymers with very low PSu content does the Baur model rather than the Flory model fit the experiment, showing that the comonomer exclusion model may hold. The deviation is more obvious as the comonomer content increases. Consequently, comonomer exclusion alone cannot account for the observed melting-point depression.

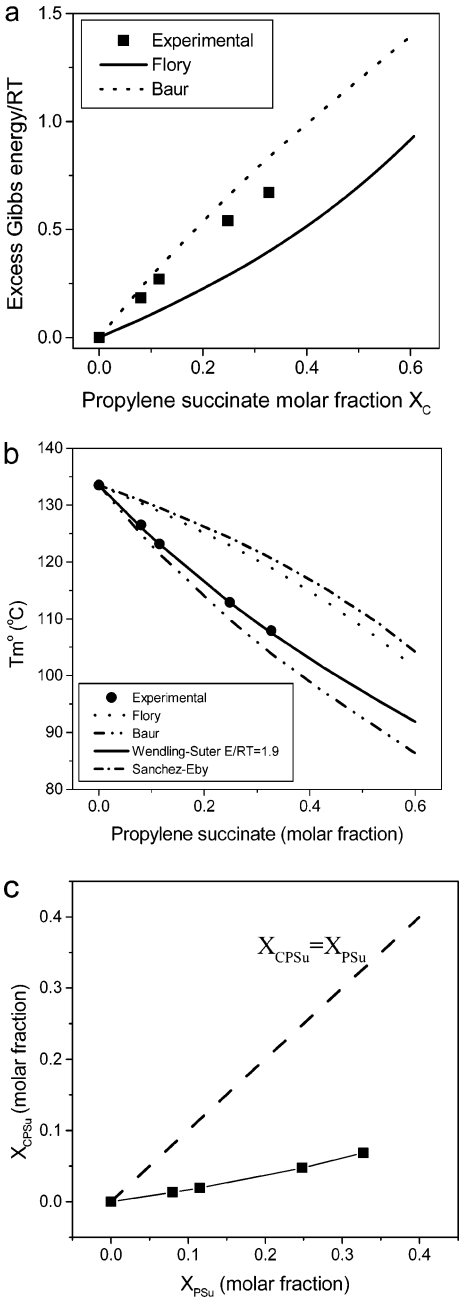

Figure 9. (a) Excess Gibbs energy/RT as obtained from experiment and from Flory and Baur models, (b) comparison of the theoretical melting temperatures and experimental values, and (c) equilibrium concentrations of PSu units in PBSu crystal as a function of copolymer composition.

In Figure 9b, the equilibrium melting temperatures calculated using the Flory, Baur, Sanchez−Eby and Wendling−Suter equations are shown in comparison to the "experimental" values obtained from the Hoffman−Weeks method. The Flory and Sanchez−Eby models lead to an overestimation of the equilib-

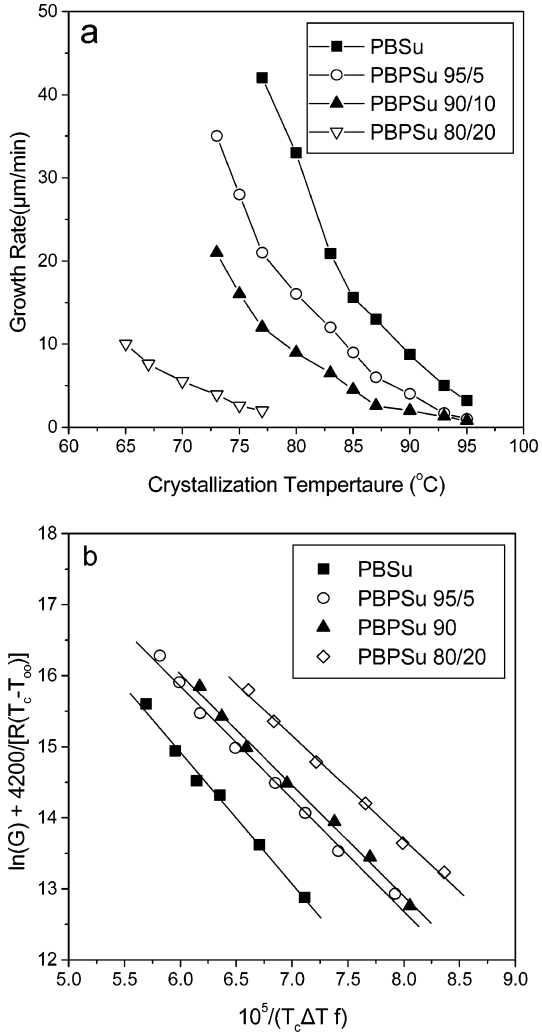

Figure 10. (a) Spherulite growth rates as a function of temperature and (b) Lauritzen−Hoffman plots for PBSu- and BSu-rich copolymers.

rium melting points. Although the Baur prediction is more realistic, the resulting values are lower than the experimental values. The Wendling−Suter model fits better to the experimental data. The value of the function $\in/RT$ is determined as an adjustable parameter. The model gives the constant $\in/RT$ value regardless of the comonomer composition. In calculations, a value of 36 kJ/mol was supposed for the equilibrium melting enthalpy.[13] The best fit to the experimental data was for $\in/RT = 1.9$ for PBSu. When the average defect free energy in the case of the incorporation of a PSu unit into the PBSu crystal was calculated from the value of $\in/RT$ for PBSu ($X_{PSu} = 0$), it was found that $\in = 6.42$kJ/mol. The experimental data at low comonomer concentrations are fitted best if a larger $\in/RT$ value is used. However, the excess free energy decreases with increasing comonomer content. This indicates that the comonomer inclusion is favored for copolymers with high comonomer content.

Using eq 9 the equilibrium concentrations X_{CPSu} of comonomer units in the crystals were estimated. The plot of the equilibrium concentration of PSu units in PBSu crystal (X_{CPSu}) versus the concentration of PSu units in the copolymer (X_{PSu}) is shown in Figure 9c. It is revealed that the comonomer concentration in crystals increases upon increasing the comonomer composition in bulk. However, the comonomer concentration in crystal is lower than the copolymer concentration in the uniform inclusion model $X_{CPSu} = X_{PSu}$. The plot of X_{CPSu} versus X_{PSu} is not linear, and it has an increasing slope. The physical

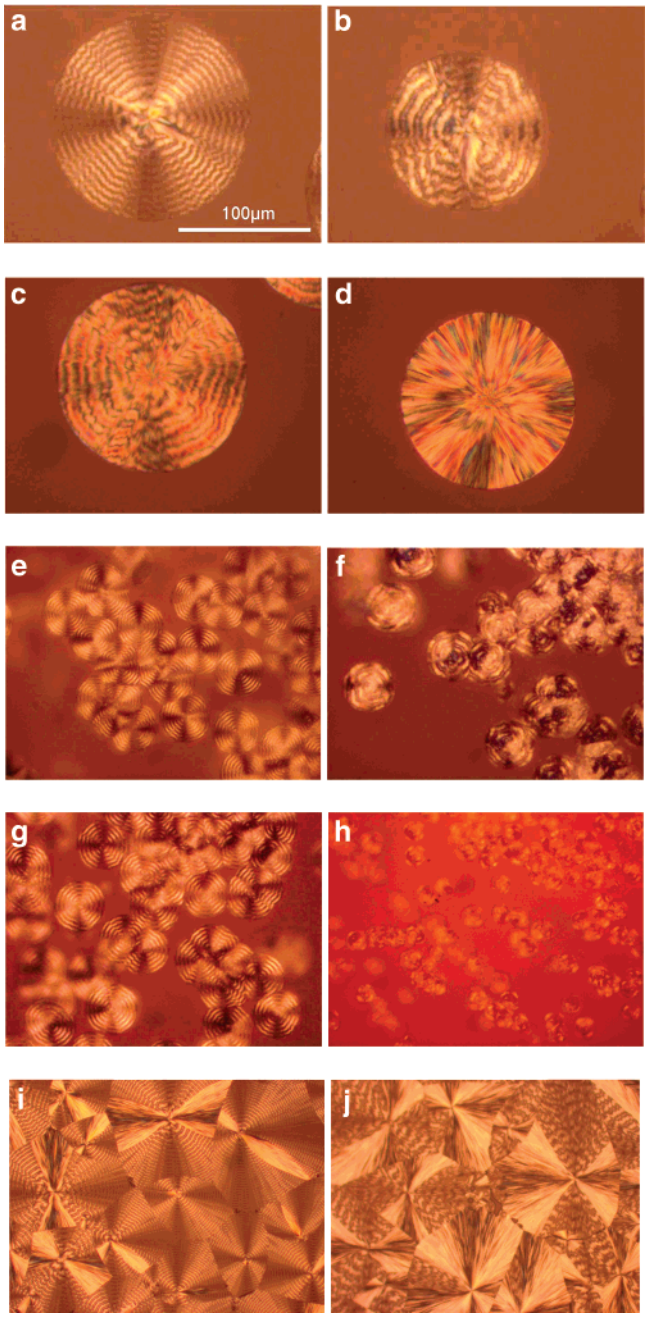

Figure 11. POM photographs showing spherulites for (a) PBPSu 95/5 at 70 °C, (b) PBPSu 95/5 at 75 °C, (c) PBPSu 95/5 at 80 °C, (d) PBPSu 95/5 at 85 °C, (e) PBPSu 70/30 at 50 °C, (f) PBPSu 70/30 at 60 °C, (g) PBPSu 60/40 at 45 °C, (h) PBPSu 40/60 at 25 °C, (i) PBSu at 70 °C, and (j) PBSu at 80 °C. The scale is the same for all photos.

meaning of this fact is that it is easier to create the excess volume necessary for a comonomer unit in an already imperfect crystal lattice.[50]

The results of the above WAXD and melting-point depression studies show isodimorphism. For the copolymers forming PBSu crystals, it seems that a portion of the PSu comonomer units, at least for large comonomer contents, are incorporated into the crystal lattice of PBSu. The opposite was not evidenced. As a matter of fact, BSu units are bulkier. In general, the incorporation of the bulkier comonomer units into the crystal of the homopolymer corresponding to the other monomer is sterically hindered. Cocrystallization is a topic with increasing interest, especially for biodegradable copolymers. In past years, the solid state of poly(3-hydroxy butyrate) copolymers and blends has been studied using solid-state NMR.[71−75] Also, the cocrystal-

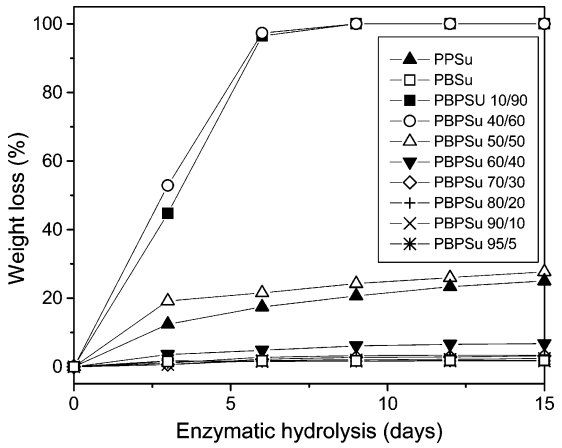

Figure 12. Weight loss as a function of time of enzymatic hydrolysis for PBPSu copolyesters.

lization behavior of adipate copolymers has been studied recently with solid-state NMR, but contradictory results were reported. It seems that more research is needed.[76−79]

Spherulitic Growth Rate. The spherulitic growth rates of PBSu and copolymers with more than 30 mol % BSu content were studied. According to the secondary nucleation theory of Lauritzen and Hoffman, the spherulitic growth rates can be expressed as[80]

$$G = G_o \exp\left[\frac{-U^*}{R(T_c - T_\infty)}\right] \exp\left[\frac{-K_g}{T_c(\Delta T)f}\right] \qquad (12)$$

where G_o is a pre-exponential factor independent of temperature. The first exponential term in the above equation contains the contribution of the diffusion process to the growth rate, where U^* is the activation energy of the molecular transfer through the melt−crystal interface, T_∞ is the temperature below which diffusion stops, and R is the gas constant. The second exponential term is the contribution of the nucleation process, where K_g is the activation energy for nucleation for a crystal with a critical size and strongly depends on the degree of supercooling ($\Delta T = T_m^o - T_c$), and f is a correction factor for the temperature dependence of the enthalpy of fusion, which is close to unity at high temperatures [$f = 2T_c/(T_m + T_c)$]. In order to obtain the best fit for the secondary nucleation theory, two parameters should be predefined: the equilibrium melting temperature and the equilibrium melting enthalpy. These were assumed to be $T_m^o = 133.5$ °C and $\Delta H_m^o = 281.4 \times 10^6$ J/m^3 for PBSu.[13] For the BSu-rich copolymers, the respective T_m^o values reported in Table 2 were used in this analysis.

Generally, eq 12 is rewritten in a logarithmic form as follows:

$$\log G + \left[\frac{-U^*}{2.303R(T_c - T_\infty)}\right] = \log G_o - \frac{K_g}{2.303T_c(\Delta T)f} \qquad (13)$$

The parameter K_g contains the variable n, reflecting the regime behavior. K_g is given by

$$K_g = \frac{nb_o\sigma\sigma_e T_m^o}{\Delta H_m^o k} \qquad (14)$$

where n is a constant equal to 4 for regimes I and III and 2 for regime II, b_o is the molecular thickness, σ is the lateral surface free energy, σ_e is the fold surface free energy, and k is the Boltzmann constant.[80] As was reported in the section for the estimation of T_m^o, the Hoffman−Weeks method is based on an equation that was deduced from a combination of the Gibbs−Thomson equation and secondary nucleation theory. Equation 14 shows the correlation between K_g and T_m^o.

The spherulite growth rates of PBSu and the 95/5, 90/10, and 80/20 copolymers were obtained from PLM measurements and can be seen in Figure 10a. They were analyzed with eq 13 to estimate the Lauritzen−Hoffman parameters. The best set of U^*,T_∞ parameters for PBSu was found to be $U^* = 4200$ cal/mol (17 590 J/mol) and $T_\infty = (T_g - 51.6)$ K. Figure 10b shows the Lauritzen−Hoffman plots for the copolymers and PBSu. It was found that, for PBSu crystallization, regime transition II → III occurs at 96 °C, in accordance with the results of previous works.[13,22] In this research, the spherulite growth rates at lower temperatures were analyzed, assuming regime III, and the same was also supposed for the copolymers. For copolymers, tests were carried out at lower temperatures corresponding to about the same supercoolings. The analysis resulted in the K_g values summarized in Table 2. As one can see, the trend for K_g was to reduce slightly with comonomer content in the copolyesters. Similar behavior has also been observed in previous studies of other types of PBSu copolymers.[21,22]

The spherulitic morphologies of PBSu and the copolymers with more than 40 mol % BSu content were observed after isothermal crystallization or cooling from the melt. The size of the spherulites increased with the crystallization temperature, as a result of reduced nucleation rate and, consequently, lower nucleation density. Banded spherulites were observed for the copolyesters and the neat polymer. The spacing of the bands increased with increasing crystallization temperature. Figure 11 shows some photographs taken with PLM. As can be seen for the PBPSu 95/5 copolymer, the band spacing steadily increased with crystallization temperature. It is important to say that banded spherulites were clearly observed even for the PBPSu 50/50. According to Woo et al., a possible origin of ring bands can be described through combined mechanisms of waving (zigzagging) and twisting (spiraling) of the lamellae during crystallization.[81] The magnitude of the spherulites, however, decreased for the PBPSu 40/60. Also, the brightness and the colors of the spherulites significantly decreased for high comonomer unit content. Finally, it is important to report that, for low molecular weight PBSu samples, which were also studied in this work, petal-like textures were observed. In these textures, no bands were observed. With increasing temperature, the petals turned to condense maltese crosses, and, in the directions where bands remained, the band spacing increased and finally disappeared. Similar textures were reported by Doi et al. for a poly(butylene-*co*-ethylene succinate) copolyester with 14 mol % ethylene succinate content.[24]

Enzymatic Hydrolysis Studies. It is well-known that the biodegradation rates of aliphatic polyesters depend on many factors such as the degree of crystallinity and molecular mobility. PPSu, as was found in our previous study, shows faster biodegradation than PBSu.[40] The weight loss of neat polyesters, in comparison with their copolymers during enzymatic hydrolysis for several days, is presented in Figure 12. As can be seen, the biodegradation rate for PBSu is negligible up to 15 days of enzymatic hydrolysis since the maximum weight loss is very small (about 2 wt %). On the other hand, PPSu has a higher biodegradation rate with a weight loss close to 25 wt % for the same time. This is expected since PPSu is less crystalline than PBSu, and, additionally, its ester bond density is higher than that of PBSu for the same molar fraction. This is in accordance

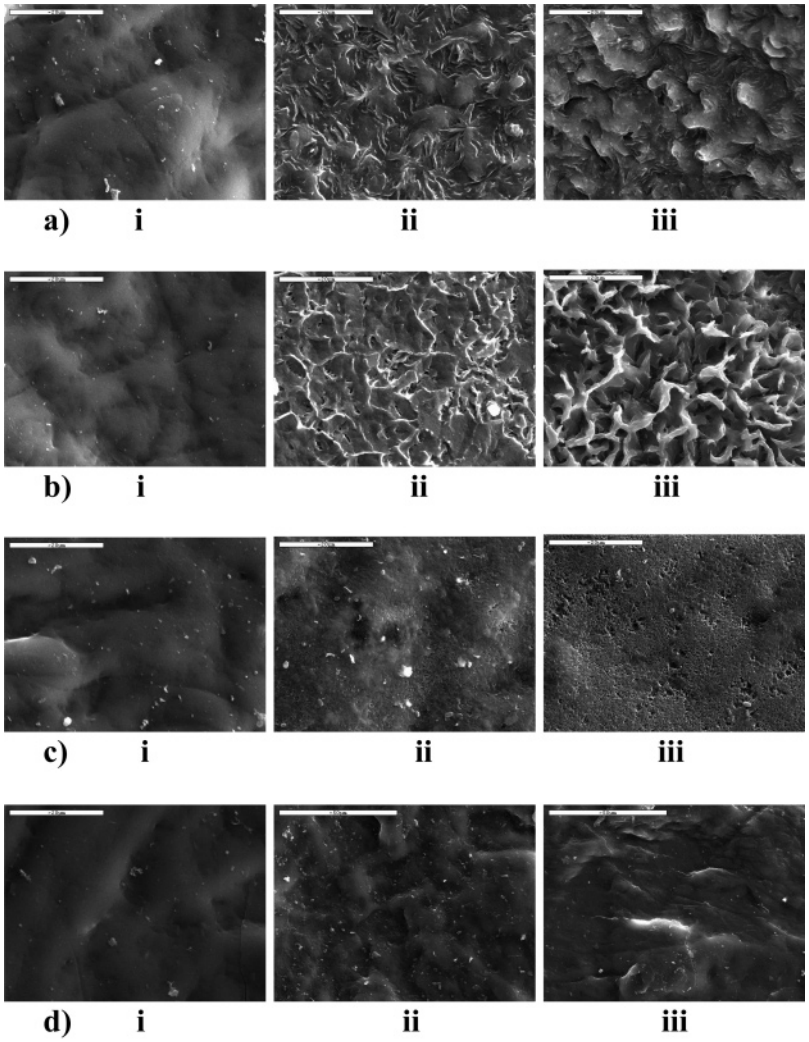

Figure 13. SEM micrographs of PBPSu copolymers during enzymatic hydrolysis at several times: (a) PBPSu 10/90 at (i) 0 days, (ii) 3 days, and (iii) 6 days; (b) PBPSu 40/60 at (i) 0 days, (ii) 3 days, and (ii) 6 days; (c) PBPSu 70/30 at (i) 0 days, (ii) 6 days, and (iii) 15 days; and (d) PBPSu 90/10 at (i) 0 days, (ii) 6 days, and (iii) 15 days.

with a recent study of Herzog et al., where it was proved by using amorphous polyester nanoparticles that polymer structure and mainly the ester bond density have a direct influence on enzymatic hydrolysis.[82] They reported that, as the ester bond density increases up to 12−13 mmol/cm^3, the degradation rate increases, and, after that, the value reaches a plateau. The copolymers containing high amounts of BSu units follow the enzymatic hydrolysis behavior of neat PBSu, showing slow degradation. Thus, for BSu unit contents ranging from 60 to 90 mol %, the weight loss ranges between 3 and 7 wt %. On the contrary, the copolymers containing more than 50 mol % PSu units seem to degrade faster, not only compared with the aforementioned copolymers, but also compared with the neat PPSu. Especially, the PBPSu 10/90 and 40/60 copolymers degrade completely after 9 days of enzymatic hydrolysis. Such higher rates were unexpected; instead a maximum weight loss at the level of neat PPSu would be anticipated. One possible explanation for such behavior could be that these copolymers have a lower degree of crystallinity than the neat PPSu. It is well-known that copolymers with a low degree of crystallinity degrade faster.[83,84] WAXD patterns of these PBPSu copolymers (Figure 7a and Table 1) revealed that indeed they have lower crystallinity. Also, these copolyesters have lower melting points than PPSu. Marten et al. reported recently that the mobility of polyester chains and mainly their melting points are the main factors that influence the enzymatic hydrolysis rates of aliphatic polyesters and their copolymers[85,86] An additional factor could be the different molecular weights of the polyesters. However, as can be seen in Table 1, neat PPSu has a lower molecular weight compared with that of the copolymers. Furthermore, lipases are endo-type enzymes degrading the ester bonds of macromolecular chains randomly, and, for this reason, variations in molecular weight do not affect biodegradation rate. Therefore, the different biodegradation rates of the studied copolymers must be attributed to the different degrees of crystallinity and their lower melting points. Finally, apart from the lower crystallinity, the morphology, meaning the small and defective crystals, the reduced spherulite size, and also the characteristics and the composition of the amorphous phase, which are probably less constraint for copolymers, might also play a role. Since for copolymers forming PBSu crystals, the mole fraction of PSu, which is incorporated in PBSu crystals, is lower than the bulk concentration, the amorphous phase is enriched in PSu units. However, the mobility of the copolymer amorphous phase is increased because of the occurrence of some longer and flexible BSu units remaining in the noncrystallizing segments. Also, in general, both crystalline and amorphous phases are less ordered for the copolymers compared to the corresponding phases of a homopolymer. This might promote degradation of the amorphous phase.

Weight loss gives a general trend for the rate of enzymatic hydrolysis, but it is not possible to find out how this hydrolysis

proceeds from weight loss alone. For this reason, morphological examinations are necessary. SEM micrographs of PBPSu copolymers after enzymatic hydrolysis for various times are presented in Figure 13. As can be seen, each copolymer shows different behavior depending on the PSu content, as was found from weight loss measurements. For the PBPSu 10/90 and 40/60 copolymers, which showed large mass loss even from the first 3 days of enzymatic hydrolysis, large parts of the film surface were removed, and, after 6 days, small fragments due to extended surface erosion were revealed (Figure 13a,b). On the other hand, the rate of mass subtraction was smaller in the copolymers with 30 mol % PSu, and thus only small holes were created on the film surface (Figure 13c). Furthermore, in the copolymer with the lowest PSu content (PBPSu 90/10), the surface erosion was negligible, in agreement with the low mass loss observed.

Conclusions

WAXD studies proved that, even for a 60 mol % PSu content, the PBPSu copolymers crystallize forming PBSu crystals. In contrast, for an 88.5 mol % PSu content, the particular copolymer formed PPSu crystals. Also, a systematic melting-point depression was observed. This fact evidenced isodimorphic cocrystallization.

The Wendling−Suter model for the analysis of the melting point depression in the case of the PBPSu copolymers, showed an increasing probability of PSu units to be incorporated in the PBSu crystals with increasing PSu unit content in the copolymer. However, only a small fraction of the comonomer units is incorporated in the crystals.

Reduced crystallinity and multiple melting behavior were observed for copolymer samples isothermally crystallized. A higher portion of secondary crystals was observed for copolymers with higher comonomer content, as well as broader melting peaks and the absence of recrystallization exotherms.

The copolymers formed banded spherulites, with increasing band spacing with crystallization temperature.

The most important feature was that the copolymers with high PSu content showed faster enzymatic degradation rates, most probably associated with their reduced crystallinity, and lower melting points. Also, the ester bond density might play a role.

Acknowledgment. This work was funded by the Greek Ministry of Education through the postdoctoral research program EPEAEK Pythagoras I.

References and Notes

(1) Rizzarelli, P.; Puglisi, C.; Montaudo, G. *Polym. Degrad. Stab.* **2004**, *85*, 855.
(2) Avella, M.; Martuscelli, E.; Raimo, M. *J. Mater. Sci.* **2000**, *35*, 523.
(3) Schmid, M.; Ritter, A.; Gubelnik, A.; Zinn, M. *Biomacromolecules* **2007**, *8*, 579.
(4) Zinn, M.; Witholt, B.; Egli, T. *Adv. Drug Delivery Rev.* **2001**, *53*, 5.
(5) Kumagai, Y.; Doi, Y. *Polym. Degrad. Stab.* **1992**, *36*, 241.
(6) Ihn, K. J.; Yoo, E. S.; Im, S. S. *Macromolecules* **1995**, *28*, 2460.
(7) Ichikawa, Y.; Kondo, H.; Igarashi, Y.; Noguchi, K.; Okuyama, K.; Washiyama, J. *Polymer* **2000**, *41*, 4719.
(8) Ichikawa, Y.; Suzuki, J.; Washiyama, J.; Moteki, Y.; Noguchi K.; Okuyama K. *Polymer* **1994**, *35*, 3338.
(9) Miyata, T.; Masuko, T. *Polymer* **1997**, *39*, 1399.
(10) Yasuniwa, M.; Satou, T. *J. Polym. Sci., Part B: Polym. Phys.* **2002**, *40*, 2411.
(11) Yasuniwa, M.; Tsubakihara, S.; Satou, T.; Iura, K. *J. Polym. Sci., Part B: Polym. Phys.* **2005**, *43*, 2039.
(12) Yoo, E. S.; Im, S. S. *J. Polym. Sci., Part B: Polym. Phys.* **1999**, *37*, 1357.
(13) Papageorgiou, G. Z; Bikiaris, D. N. *Polymer* **2005**, *46*, 12081.
(14) Qiu, Z.; Komura.; Ikehara, T.; Nishi, T. *Polymer* **2003**, *44*, 7781.
(15) Mochizuki, M.; Mukai, K.; Yamada, K.; Ichise, N.; Murase, S.; Iwaya, Y. *Macromolecules* **1997**, *30*, 7403.
(16) Li, F.; Xu, X.; Hao, Q.; Li, Q.; Yu, J.; Cao, A. *J. Polym. Sci., Part B: Polym. Phys.* **2006**, *44*, 1635.
(17) Nagata, M.; Goto, H.; Sakai, W.; Tsutsumi, N. *Polymer* **2000**, *41*, 4373.
(18) Ahn, B. D.; Kim, S. H.; Yang, J. S. *J. Appl. Polym. Sci.* **2001**, *82*, 2808.
(19) Yang, J.; Tian, W.; Li, Q.; Cao, A. *Biomacromolecules* **2004**, *5*, 2258.
(20) Zhang, S.; Yang, J.; Liu, X.; Chang, J; Cao, A. *Biomacromolecules* **2003**, *4*, 437.
(21) Park, J. W.; Kim, D. K.; Im, S. S. *Polym. Int.* **2002**, *51*, 239.
(22) Gan, Z.; Abe, H.; Kurokawa, H.; Doi, Y. *Biomacromolecules* **2001**, *2*, 605.
(23) Liu, X.; Li, C.; Zhang, D.; Xiao, Y. *J. Polym. Sci., Part B: Polym. Phys.* **2006**, *44*, 900.
(24) Gan, Z; Abe, H.; Doi, Y. *Biomacromolecules* **2001**, *2*, 313.
(25) Qiu, Z.; Ikehara, T.; Nishi, T. *Polymer* **2003**, *44*, 7519.
(26) Qiu, Z.; Komura, M.; Ikehara, T.; Nishi, T. *Polymer* **2003**, *44*, 7749.
(27) Qiu, Z.; Ikehara, T.; Nishi, T. *Polymer* **2003**, *44*, 2503.
(28) Qiu, Z.; Komura, M.; Ikehara, T.; Nishi, T. *Polymer* **2003**, *44*, 8111.
(29) Papageorgiou, G. Z; Bikiaris, D. N. *J. Polym. Sci., Part B: Polym. Phys.* **2005**, *44*, 584.
(30) Okata, T.; Lee, S. H. *J. Appl. Polym. Sci.* **2005**, *97*, 1107.
(31) Yoo, E. S.; Im, S. S. *J. Environ. Polym. Degrad.* **1999**, *7*, 19.
(32) Chrissafis, K.; Paraskevopoulos, K. M.; Bikiaris, D. N. *Thermochim. Acta* **2005**, *435*, 342.
(33) Ranucci, E.; Söderqvist Lindblad, M.; Albertsson, A. C. *Macromol. Rapid Commun.* **2000**, *21*, 680.
(34) Liu, Y.; Ranucci, E.; Söderqvist Lindblad, M.; Albertsson, A. C. *J. Polym. Sci., Part A: Polym. Chem.* **2001**, *39*, 2508.
(35) Wang, B.; Li, C. Y.; Hanzlicek, J.; Cheng, S. Z. D.; Geil, P. H.; Grebowicz, J.; Ho, R. M. *Polymer* **2001**, *42*, 7171.
(36) Karayannidis, G.; Roupakias, C.; Bikiaris, D.; Achilias, D. *Polymer* **2003**, *44*, 931.
(37) Hartlep, H.; Hussmann, W.; Prayitno, N.; Meynial-Salles, I.; Zeng, A. P. *Appl. Microbiol. Biotechnol.* **2002**, *60*, 60.
(38) Kim, D. Y.; Yim, S. C.; Lee, P. C.; Lee, W. G.; Lee, S. Y.; Chang, H. N. *Enzyme Microb. Technol.* **2004**, *35*, 648.
(39) Liu, Y.; Söderqvist Lindblad, M.; Ranucci, E.; Albertsson, A. C. *J. Polym. Sci., Part A: Polym. Chem.* **2001**, *39*, 630.
(40) Bikiaris, D. N.; Papageorgiou, G. Z.; Achilias, D. S. *Polym. Degrad. Stab.* **2006**, *91*, 31.
(41) Umare, S. S.; Chandure, A. S.; Padney, R. A. *Polym. Degrad. Stab.* **2007**, *92*, 464.
(42) Soccio, M.; Nogales, A.; Lotti, N.; Munari, A.; Ezquerra, T. A. *Phys. Rev. Lett.* **2007**, *98*, 37801.
(43) Chrissafis, K.; Paraskevopoulos, K. M.; Bikiaris, D. N. *Polym. Degrad. Stab.* **2006**, *91*, 60.
(44) Soccio, M.; Finelli, L.; Lotti, N.; Gazzano, M.; Munari, A. *J. Polym. Sci., Part B: Polym. Phys.* **2007**, *45*, 310.
(45) Xu, Y.; Xu, J.; Guo, B.; Xie, X. *J. Polym. Sci., Part B: Polym. Phys.* **2007**, *45*, 420.
(46) Bikiaris, D. N.; Achilias, D. S. *Polymer* **2006**, *47*, 4851.
(47) Allegra, G.; Bassi, I. W. *Adv. Polym. Sci.* **1969**, *6*, 549.
(48) Lee, J. H.; Jeong, Y. G.; Lee, S. C.; Min, B. G.; Jo, W. H. *Polymer* **2002**, *43*, 5263.
(49) Orts, W. J.; Marchessault, R. H.; Bluhm, T. L. *Macromolecules* **1991**, *24*, 6435.
(50) VanderHart, D. L.; Orts, W. J.; Marchessault, R. H. *Macromolecules* **1995**, *28*, 6394.
(51) Papageorgiou, G. Z.; Achilias, D. S.; Karayannidis, G. P. *Polym. Int.* **2004**, *53*, 360.
(52) Jeong, Y. G.; Jo, W. H.; Lee, S. C. *Macromolecules* **2000**, *33*, 9705.
(53) Flory P. J. *J. Chem. Phys.* **1947**, *15*, 684.
(54) Flory P. J. *Trans. Faraday Soc.* **1955**, *51*, 848.
(55) Baur, V. H. *Makromol. Chem.* **1966**, *98*, 297.
(56) Sanchez, I. C.; Eby, R. K. *Macromolecules* **1975**, *8*, 638.
(57) Wendling, J.; Gusev, A. A.; Suter, U. W. *Macromolecules* **1998**, *31*, 2509.
(58) Wendling, J.; Suter, U. W. *Macromolecules* **1998**, *31*, 2516.
(59) Wendling, J.; Gusev, A. A.; Suter, U. W.; Braam, A.; Leemans, L.; Meier, R. J.; Aerts, J.; Heuvel, J.; Hottenhuis, M. *Macromolecules* **1999**, *32*, 7866.
(60) Kilian, H. G. *Kolloid Z. Z. Polym.* **1965**, *202*, 97.
(61) Helfand, E.; Lauritzen, J. I. *Macromolecules* **1973**, *6*, 631.
(62) Crist, B. *Polymer* **2003**, *44*, 4563.
(63) Goldbeck-Wood, G. *Polymer* **1992**, *33*, 778.

(64) Fox, G. *Bull. Am. Chem. Soc*. **1956**, *1*, 123.
(65) Papageorgiou, G. Z.; Karayannidis, G. P. *Polymer* **1999**, *40*, 5325.
(66) Sauer, B. B.; Kampert, W. G.; Neal Blanchard, E.; Threefoot, S. A.; Hsiao, B. S. *Polymer* **2000**, *41*, 1099.
(67) Jourdan, N.; Deguire, S.; Brisse, F. *Macromolecules* **1995**, *28*, 8086.
(68) Hay, J. N.; Langford, J. I.; Lloyd, J. R. *Polymer* **1989**, *30*, 489.
(69) Xu, J.; Srivatsan, S.; Marand, H.; Agarwal, P. *Macromolecules* **1998**, *31*, 8230.
(70) Hoffman, J. D.; Weeks, J. *J. Res. Natl. Bur. Stand.* **1962**, *66A*, 13.
(71) Yoshie, N.; Saito, M.; Inoue, Y. *Macromolecules* **2001**, *34*, 8953.
(72) Zhang, L.; Tang, H.; Hou, G.; Shen, Y.; Deng, F. *Polymer* **2007**, *48*, 2928.
(73) Shuai, X.; Porbeni, F. E.; Wei, M.; Bullions, T.; Tonelli, A. E. *Macromolecules* **2002**, *35*, 3126.
(74) Reeve, M. S.; McCarthy, S. P. J.; Gross, R. A. J. *Macromolecules* **1993**, *26*, 888.
(75) Koyama, N.; Doi, Y. *Macromolecules* **1996**, *29*, 5843.
(76) Cranston, E.; Kawada, J.; Raymond, S.; Morin, F.; Marchessault, R. *Biomacromolecules* **2003**, *4*, 995.
(77) Kuwabara, K.; Gan, Z.; Nakamura, T.; Abe, H.; Doi, Y. *Biomacromolecules* **2002**, *3*, 390.
(78) Shi, X. Q.; Aimi, K.; Ito, H.; Ando, S.; Kikutani, T. *Polymer* **2005**, *46*, 751.
(79) Shi, X. Q.; Ito, H.; Kikutani, T. *Polymer* **2005**, *46*, 11442.
(80) Hoffman, J. D.; Davis, G. T.; Lautitzen, J. I., Jr. In *Treatise on Solid State Chemistry: Crystalline and Noncrystalline Solids*; Hannay, N. B., Ed.; Plenum Press: New York, 1976; Vol. 3, Chapter 7.
(81) Wu, P. L.; Woo, E. M.; Liu, H. L. *J. Polym. Sci., Part B: Polym. Phys.* **2004**, *42*, 4421.
(82) Herzog, K.; Müller, R. J.; Deckwer, W. D. *Polym. Degrad. Stab.* **2006**, *91*, 2486.
(83) Yuan, M.; Wang, Y.; Li, X.; Xiong, C.; Deng, X. *Macromolecules* **2000**, *33*, 1613.
(84) Seretoudi, G.; Bikiaris, D.; Panayiotou, C. *Polymer* **2002**, *43*, 5405.
(85) Marten, E.; Müller, R. J.; Deckwer, W. D. *Polym. Degrad. Stab.* **2003**, *80*, 485.
(86) Marten, E.; Müller, R. J.; Deckwer, W. D. *Polym. Degrad. Stab.* **2005**, *88*, 371.

BM0703113